

Charged qOS-extremal black hole and its scalarization by entropy function approach

Yun Soo Myung*

Center for Quantum Spacetime, Sogang University, Seoul 04107, Republic of Korea

Abstract

We investigate scalarization of charged quantum Oppenheimer-Snyder extremal (cqOSe)-black hole in the Einstein-Gauss-Bonnet-scalar theory with a nonlinear electrodynamics term. This black hole is described by quantum parameter α and magnetic charge P . It is equivalent to the qOS-extremal black hole whose action is still unknown when imposing a relation of $(3\alpha P^2)^{1/4} \rightarrow 3M/2$. Focusing on the onset of scalarization, we find the single branch of scalarized cqOS extremal (scqOSe)-black holes. To obtain a scalar cloud (seed) for the single branch, however, we have to consider its near-horizon geometry of the Bertotti-Bobinson (BR) spacetime. In this case, two scalar clouds for positive and negative coupling constant λ are found to represent two branches. Applying Sen's entropy function approach to this theory, we obtain the entropy which is the only physical quantity to describe the scqOSe-black holes. We find that the positive branch is preferred than the negative branch.

Typeset Using L^AT_EX

*e-mail address: ysmyung@inje.ac.kr

1 Introduction

The quantum Oppenheimer-Snyder (qOS)-black hole was recently found by considering the qOS model in loop quantum cosmology [1]. The qOS model describes a collapsing dust ball inside the qOS-black hole, while the quantum Swiss Cheese model describes the qOS-black hole surrounded by Ashtekar-Pawlowski-Singh model [2]. However, one does not know its action \mathcal{L}_{qOS} to give the qOS-black hole described by mass (M) and quantum parameter (α) as a direct solution. Regarding to appropriate actions for \mathcal{L}_{qOS} , a candidate was proposed by introducing a nonlinear electrodynamics (NED) term \mathcal{L}_{NED} [3]. In this case, one has found charged quantum Oppenheimer-Snyder(cqOS)-black hole and the qOS-black hole can be recovered when choosing $P = M$. Various aspects of the qOS-black hole have been studied by including quasinormal mode analysis for tensor and scalar perturbations [4], thermodynamics [5, 6], shadow radius [7, 8], and scalarization within the Einstein-Gauss-Bonnet-scalar (EGBS) theory [9, 10].

On the other hand, extremal black holes have played a crucial role in various aspects. They possessing zero Hawking temperature and heat capacity, are expected to bring us valuable insights into black hole thermodynamics [11] and Hawking radiation [12]. For these black holes, hence, the entropy is regarded as the only physical quantity. In the astrophysical aspect, many astrophysical black holes are supposed to be nearly extremal [13, 14]. To understand the nature of extremal black holes, one has to study the dynamical properties of test fields propagating around them but it requires the investigation to confine to the near-extremal limit or the near-horizon approximation.

In addition, the no-hair theorem states that a black hole can be completely described by three parameters: mass (M), electric charge (Q), and rotation parameter (a) in Einstein-Maxwell gravity [15, 16]. If a scalar field is minimally coupled to gravitational and electromagnetic fields, it turned out that there is no black hole solution with scalar hair [17]. However, its evasion occurred frequently in the context of scalar-tensor theories with the nonminimal scalar coupling either to Gauss-Bonnet (GB) term [18, 19, 20] or to Maxwell term [21, 22]. The former is called GB^+ scalarization with a positive coupling parameter and the latter is called M^+ scalarization, both were triggered by tachyonic instability. Here, one found infinite branches of scalarized black holes induced by infinite scalar clouds. For review on spontaneous scalarization, one may see Ref. [23].

The GB^- scalarization can be realized for the black hole with double horizons when

coupling $f(\phi)$ to the GB term with negative coupling parameter. It was shown that two branches of positive ($\gamma > 0$) and negative ($\gamma < 0$) coupling parameter are allowed for scalarization of the Reissner-Nordström (RN) black holes in the Einstein-Gauss-Bonnet-Naxwell-scalar (EGBMS) theory with coupling function $f(\phi) = \gamma\phi^2$ [24]. It was claimed that the appearance of negative branch is related to its near-horizon geometry ($\text{AdS}_2 \times S^2$) of extremal RN black hole. However, the negative branch appeared from the sign change of GB term [25]. For qOS-extremal black holes, its scalar potential has a negative region in the whole near-horizon [26]. This is the origin of GB^- scalarization for charged black holes with negative coupling constant, inducing the single branch of scalarized black holes. At this stage, one has to realize that it is not easy to obtain its scalar cloud, which may be a seed to generate the single branch of scalarized extremal black holes. This is because numerical methods cannot solve the linearized scalar equation to find out scalar clouds in the extremal black hole background [27, 28]. It forces the numerical investigation to end at the near-extremal limit [29] or at the near-horizon approximation. To obtain the scalar clouds, here, one may use the near-horizon geometry [Bertotti-Bobinson (BR: $\text{AdS}_2 \times S^2$) spacetime] of extremal black holes.

In the present work, we wish to investigate GB^- scalarization of cqOSe-black hole in the EGBS theory with the NED term \mathcal{L}_{NED} and the coupling function $f(\phi) = 2(\lambda\phi^2 - \zeta\phi^4)$ to GB term. Here, λ and ζ represent two scalar coupling parameters. This extremal black hole is described by two of quantum parameter α and magnetic charge P . It is equivalent to the qOS-extremal black hole whose action (\mathcal{L}_{qOS}) is still unknown when imposing a relation of $(3\alpha P^2)^{1/4} \rightarrow 3M/2$. This model suggests an alternative to studying scalarization of qOS-extremal black hole. Studying on the onset of scalarization based on the linearized theory with λ , we find the single branch of scalarized cqOS extremal (scqOSe)-black holes. To obtain a scalar cloud (seed), we consider its near-horizon geometry of the BR spacetime. Two scalar clouds are found to represent two branches. Applying Sen's entropy function approach [30] to this theory, we obtain the entropy function which indicates the only physical quantity to describe the scqOSe-black holes.

2 cqOS-extremal black hole

The EGBS theory with the nonlinear electrodynamics (NED) term takes the form [9, 10] as

$$\mathcal{L}_{\text{EGBS-N}} = \frac{1}{16\pi} \left[R - 2\partial_\mu\phi\partial^\mu\phi + f(\phi)\mathcal{R}_{\text{GB}}^2 + \mathcal{L}_{\text{NED}} \right], \quad (1)$$

where ϕ is the scalar field and $f(\phi) = 2(\lambda\phi^2 - \zeta\phi^4)$ denotes a quartic coupling function with λ and ζ scalar coupling parameters. Also, $\mathcal{R}_{\text{GB}}^2 = R^2 - 4R_{\mu\nu}R^{\mu\nu} + R_{\mu\nu\rho\sigma}R^{\mu\nu\rho\sigma}$ denotes the GB term while $\mathcal{L}_{\text{NED}} = -2\xi(\mathcal{F})^{3/2}$ represents the NED term with $\xi = \frac{3\alpha}{2^{3/2}P}$ and $\mathcal{F} = F_{\mu\nu}F^{\mu\nu}$ the Maxwell term.

The Einstein equation with $G_{\mu\nu} = R_{\mu\nu} - (R/2)g_{\mu\nu}$ is derived as

$$G_{\mu\nu} = 2\partial_\mu\phi\partial_\nu\phi - (\partial\phi)^2g_{\mu\nu} + \Gamma_{\mu\nu}^\phi + T_{\mu\nu}^{\text{NED}}, \quad (2)$$

where $\Gamma_{\mu\nu}^\phi$ with $\Psi_\mu = f'(\phi)\partial_\mu\phi$ is given by

$$\begin{aligned} \Gamma_{\mu\nu}^\phi &= 2R\nabla_{(\mu}\Psi_{\nu)} + 4\nabla^\alpha\Psi_\alpha G_{\mu\nu} - 8R_{(\mu|\alpha|}\nabla^\alpha\Psi_{\nu)} \\ &+ 4R^{\alpha\beta}\nabla_\alpha\Psi_\beta g_{\mu\nu} - 4R^{\beta}_{\mu\alpha\nu}\nabla^\alpha\Psi_\beta \end{aligned} \quad (3)$$

and the NED energy-momentum tensor takes the form

$$T_{\mu\nu}^{\text{NED}} = 6\xi \left[\sqrt{\mathcal{F}}F_{\mu\lambda}F_\nu^\lambda - \frac{1}{6}\mathcal{F}^{3/2}g_{\mu\nu} \right]. \quad (4)$$

Considering $\mathcal{F} = 2P^2/r^4$ for a magnetically charged configuration ($F_{\theta\varphi} = P \sin\theta$), its energy-momentum tensor takes the form

$$T_{\mu}^{\text{NED},\nu} = \frac{3\alpha P^2}{r^6} \text{diag}[-1, -1, 2, 2]. \quad (5)$$

In this case, choosing $P = M$ leads to the energy-momentum tensor for qOS-black hole [1]

$$T_{\mu}^{\text{qOS},\nu} = \frac{3\alpha M^2}{r^6} \text{diag}[-1, -1, 2, 2], \quad (6)$$

whose matter action is still unknown because this was derived by making use of the junction conditions. The scalar field equation is given by

$$\square\phi + \frac{1}{4}f'(\phi)\mathcal{R}_{\text{GB}}^2 = 0. \quad (7)$$

Taking into account $G_{\mu\nu} = T_{\mu\nu}^{\text{NED}}$ together with $\phi = 0$, the cqOS-black hole solution is obtained as [3]

$$ds_{\text{cqOS}}^2 = \bar{g}_{\mu\nu} dx^\mu dx^\nu = -g(r)dt^2 + \frac{dr^2}{g(r)} + r^2 d\Omega_2^2 \quad (8)$$

whose metric function is defined by the mass function $m(r)$ as

$$g(r, M, \alpha, P) \equiv 1 - \frac{2m(r)}{r} = 1 - \frac{2M}{r} + \frac{\alpha P^2}{r^4}. \quad (9)$$

Here, the quantum parameter is given by $\alpha = 16\sqrt{3}\pi\gamma^3$ with γ the dimensionless Barbero-Immirzi parameter. For $\gamma = 0.2375$, one finds that $\alpha = 1.1663$ [31, 32].

One finds two real solutions and complex solutions from $g(r) = 0$

$$r_i(M, \alpha, P), \text{ for } i = 1, 2, 3, 4, \quad (10)$$

where r_1 and r_2 become complex solutions, whereas $r_3(M, \alpha, P) \rightarrow r_-(M, \alpha, P)$ and $r_4(M, \alpha) \rightarrow r_+(M, \alpha, P)$. Their explicit forms are given by

$$\begin{aligned} r_{\pm}(M, \alpha, P) &= \frac{M}{2} + \frac{1}{2} \left[M^2 + \frac{2^{5/3}P^2\alpha}{(3\eta)^{1/3}} + \frac{(2\eta)^{1/3}}{3^{2/3}} \right]^{1/2} \\ &\pm \frac{1}{2} \left[2M^2 - \frac{2^{5/3}P^2\alpha}{(3\eta)^{1/3}} - \frac{(2\eta)^{1/3}}{3^{2/3}} + \frac{2M^3}{(M^2 + \frac{2^{5/3}P^2\alpha}{(3\eta)^{1/3}} + \frac{(2\eta)^{1/3}}{3^{2/3}})^{1/2}} \right]^{1/2} \end{aligned} \quad (11)$$

with

$$\eta(M, \alpha, P) = \alpha P^2 \left(9M^2 + \sqrt{3} \sqrt{27M^4 - 16\alpha P^2} \right). \quad (12)$$

From Eq.(12), one obtains a condition for the existence of two horizons as

$$0 < \alpha < \frac{27M^4}{16P^2}, \quad (13)$$

which leads to a cqOS-extremal black hole for $\alpha = \frac{27M^4}{16P^2}$ as

$$g_e(r, \alpha, P) = 1 - \frac{4(\alpha P^2)^{1/4}}{3^{3/4}r} + \frac{\alpha P^2}{r^4} \rightarrow \left(1 - \frac{(3\alpha P^2)^{1/4}}{r} \right)^2 \left(1 + \frac{2(\alpha P^2)^{1/4}}{3^{3/4}r} + \frac{\sqrt{\alpha P^2}}{\sqrt{3}r^2} \right). \quad (14)$$

Considering the relation $\frac{2(3\alpha P^2)^{1/4}}{3} = M$, one finds the qOS-extremal black hole solution as

$$g_{\text{qOSe}}(r, M) = 1 - \frac{2M}{r} + \frac{27M^4}{16r^4} \rightarrow \left(1 - \frac{3M}{2r} \right)^2 \left(1 + \frac{M}{r} + \frac{3M^2}{4r^2} \right). \quad (15)$$

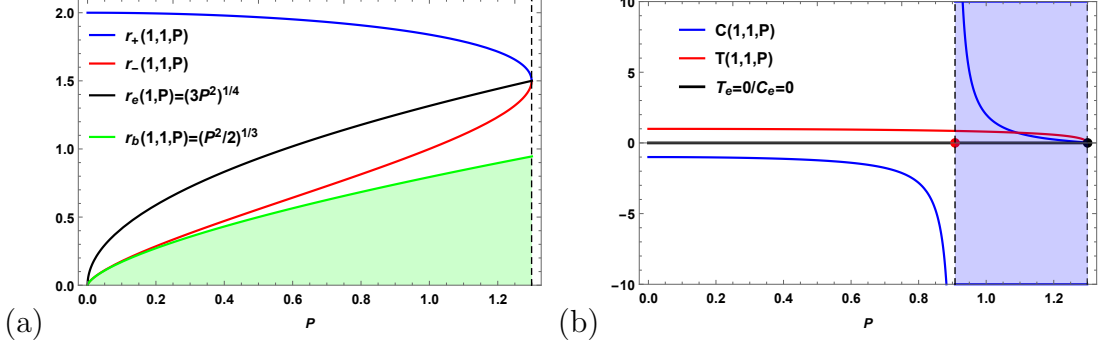


Figure 1: (a) Two horizons $r_{\pm}(M = 1, \alpha = 1, P)$ are function of $P \in [0, P_e = 1.299]$, showing the upper bound for the charge P . Here, $r_e(\alpha = 1, P)$ as a function of P represents the extremal horizon, starting from $P = 0$. The bounce radius $r_b(M = 1, \alpha = 1, P)$ is located inside the inner horizon. (b) Heat capacity $C(M = 1, \alpha = 1, P)/|C_S(1, 0)|$ with $|C_S(1, 0, 0)| = 25.13$. Heat capacity blows up at Davies point ($P_D = 0.9077$, red dot) where the temperature $T(1, 1, P)$ has the maximum. The shaded region denotes $C > 0$ for cqOSe-black holes. The heat capacity and temperature are always zero at the cqOSe-black line.

Here, we present two extremal horizons from $g_e(r) = 0$ and $g_{\text{qOSe}}(r) = 0$ as

$$r_e(\alpha, P) = (3\alpha P^2)^{1/4}, \quad r_e(M) = \frac{3M}{2}. \quad (16)$$

This shows that two extremal representations are equivalent to each other. Also, from $m(r) = 0$, one finds the bounce radius

$$r_b = \left(\frac{\alpha P^2}{2M} \right)^{1/4}, \quad (17)$$

which is located inside the inner horizon r_- (see Fig. 1(a)).

As is shown in Fig. 1(a), there exist outer/inner horizons $r_{\pm}(M = 1, \alpha = 1, P)$ as functions of P with the upper bound at $P = P_e$ for the magnetic charge of cqOSe-black hole. Also, we display the extremal horizon $r_e(\alpha = 1, P)$ as a function of P and the bounce radius $r_b(M = 1, \alpha = 1, P)$ is located inside the inner horizon.

The temperature $T = \frac{\partial m}{\partial S}$ and heat capacity $C = \frac{\partial m}{\partial r_+} \left(\frac{\partial T}{\partial r_+} \right)^{-1}$ with mass $M \rightarrow m(M, \alpha, P) =$

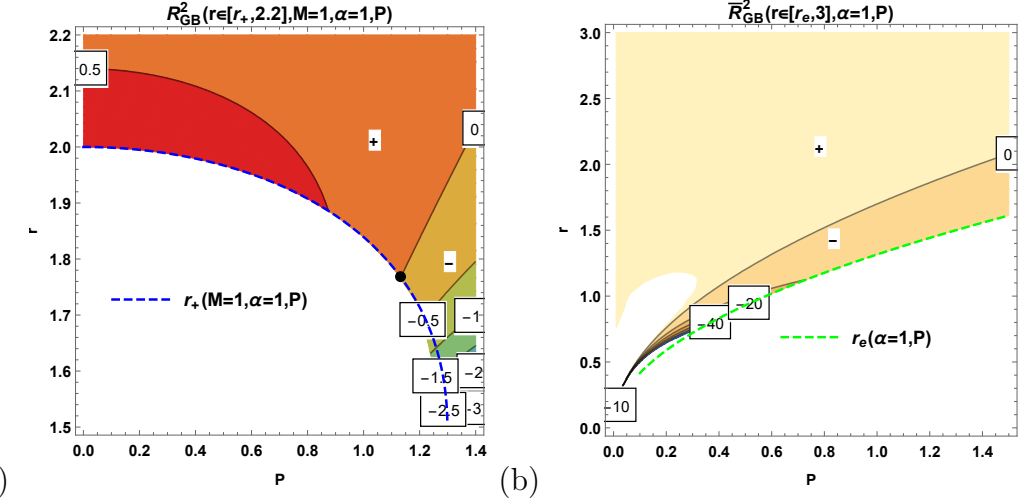


Figure 2: (a) $\mathcal{R}_{\text{GB}}^2(r, M = 1, \alpha = 1, P) < 0$ as a function of $(r \in [r_+(M = 1, \alpha = 1, P), 2.2], P \in [0, 1.5])$ in the near-horizon for cqOS black holes. Its sign changes from positive ($0 < P < P_c (= 1.1329)$) to negative ($P_c < P < P_e (= 1.299)$) with the critical onset point $[(P_c, r_+(1, 1, P_c), \text{black dot}]$. (b) $\bar{\mathcal{R}}_{\text{GB}}^2(r, \alpha = 1, P) < 0$ as a function of $(r \in [r_e(\alpha = 1, P), 3], P \in [0, 1.5])$ in the whole near-horizon for cqOSe-black holes. Hence, one finds that $-\lambda \bar{\mathcal{R}}_{\text{GB}}^2 < 0$ in the whole near-horizon for $\lambda < 0$, leading to tachyonic instability.

$(\alpha P^2 + r_+^4)/2r_+^3$ and area-law entropy $S = \pi r_+^2$ are given by

$$T(M, \alpha, P) = \frac{-3\alpha P^2 + r_+^4(M, \alpha, P)}{4\pi r_+^5(M, \alpha, P)}, \quad (18)$$

$$C(M, \alpha, P) \equiv \frac{NC(M, \alpha, P)}{DC(M, \alpha, P)} = -\frac{2\pi r_+^2(M, \alpha, P)[-3\alpha P^2 + r_+^4(M, \alpha, P)]}{-15\alpha P^2 + r_+^4(M, \alpha, P)}. \quad (19)$$

$$(20)$$

Here, the Davies point (blow-up point) can be obtained from solving $DC(M, \alpha, P) = 0$. We observe from Fig. 1(b) that $C(1, 1, P)/|C_S(1, 0, 0)|$ blows up at Davies point ($P_D = 0.9077$, red dot) where the temperature $T(M = 1, \alpha = 1, P)$ takes the maximum value. The cqOS black hole is thermodynamically stable if $C > 0$ ($P_D < P < P_e$), while it is unstable for $C < 0$ ($0 < P < P_D$). Hence, the Davies point is regarded as a critical point which can represent a sharp phase transition from $C > 0$ to $C < 0$. However, it is important to note that the temperature and heat capacity of cqOSe-black hole are always zero as is shown in the black line (Fig.1(b)), implying that the entropy survives the only physical quantity.

For cqOS black hole background, the GB term is given by

$$\mathcal{R}_{\text{GB}}^2 = \frac{48M^2}{r^6} \left[\frac{3\alpha^2 P^4}{M^2 r^6} - \frac{5\alpha P^2}{Mr^3} + 1 \right]. \quad (21)$$

The near-horizon behavior for $\mathcal{R}_{\text{GB}}^2$ is depicted in Fig. 2(a). Its sign changes from positive [$0 < P < P_c (= 1.1329)$] to negative [$P_c < P < P_e (= 1.299)$] with the critical onset point $[(P_c, r_+(1, 1, P_c)), \text{black dot}]$. This implies that GB^- scalarization is allowed only for $\lambda < 0$. It indicates that tachyonic instability of $-\lambda \bar{\mathcal{R}}_{\text{GB}}^2 < 0$ is available for $P_c < P < P_e$ (narrow strip) in the near-horizon. This corresponds to the origin for GB^- scalarization of cqOS black holes with negative λ .

3 Onset scalarization

This analysis is based on the linearized scalar theory described by

$$(\bar{\square} + \lambda \bar{\mathcal{R}}_{\text{GB}}^2) \delta\phi = 0. \quad (22)$$

3.1 GB^e scalarization for cqOSe-black hole

In this section, we wish to focus on the GB^e onset scalarization of the cqOSe-black holes. Here, we use $g_e(r, \alpha, P)$ instead of $g(r, M, \alpha, P)$, implying that it includes the degenerate horizon. In this case, its spacetime is described by

$$ds_e^2 = -g_e(r)dt^2 + \frac{dr^2}{g_e(r)} + r^2 d\Omega_2^2, \quad (23)$$

which possesses an $\text{AdS}_2 \times S^2$ as the near-horizon geometry.

Let us introduce the tortoise coordinate r_* defined as $dr_* = dr/g_e(r)$ and consider the separation of variables

$$\delta\phi(t, r_*, \theta, \varphi) = \sum_m \sum_{l=|m|}^{\infty} \frac{\psi_{lm}(t, r_*)}{r} Y_{lm}(\theta, \varphi). \quad (24)$$

Here, the radial part of the $(l = 0, m = 0)$ -linearized scalar equation takes the form

$$\frac{\partial^2 \psi_{00}(t, r_*)}{\partial r_*^2} - \frac{\partial^2 \psi_{00}(t, r_*)}{\partial t^2} = V_e(r)\psi_{00}(t, r_*), \quad (25)$$

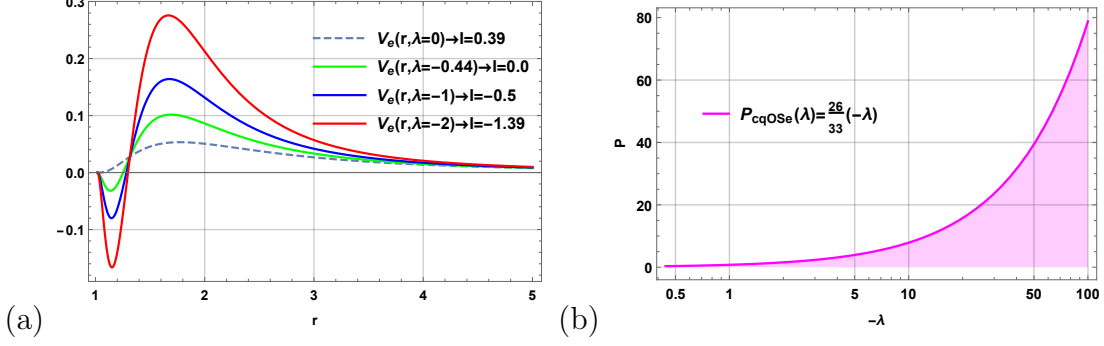


Figure 3: (a) Extremal scalar potentials $V_e(r, \alpha = 1, P = 0.6, \lambda)$ with $\lambda = 0, -0.44, -1, -2$ as a function of $r \in [r_+ = 1.019, 5]$ for GB^e scalarization. Here, one has the integration $I = 0.39(\lambda = 0)$, $0(\lambda = -0.44)$, $-0.5(\lambda = -1)$, $-1.39(\lambda = -2)$. (b) Sufficient unstable (shaded) region of cqOSe-black hole for GB^e scalarization. A single branch for $\lambda < 0$ is allowed for $0 < P < P_{\text{cqOSe}}$ ($= -0.7879\lambda$).

where the scalar potential $V_e(r)$ is given by

$$V_e(r, \alpha, P, \lambda) = g_e(r, \alpha, P) \left[\frac{4(\alpha P^2)^{1/4}}{3^{3/4} r^3} - \frac{4\alpha P^2}{r^6} + \tilde{m}_e^2 \right] \quad (26)$$

with its effective mass term

$$\tilde{m}_e^2 \equiv -\lambda \bar{\mathcal{R}}_{\text{GB}}^2 = -\frac{16\lambda}{3r^{12}} \left[27\alpha^2 P^4 - 30 \cdot 3^{1/4} (\alpha P^2)^{5/4} r^3 + 4\sqrt{3\alpha P^2} r^6 \right]. \quad (27)$$

As is shown in Fig. 2(b), the GB term $\bar{\mathcal{R}}_{\text{GB}}^2(r, \alpha = 1, P)$ is regarded as a function of $(r \in [r_+(\alpha = 1, P), 3], P \in [0, 1.5])$. Here, one observes that $\tilde{m}_e^2 < 0$ in the whole near-horizon for $\lambda < 0$, leading to tachyonic instability. Actually, Fig. 3(a) shows that the extremal potentials have negative regions in the whole near-horizon for any negative λ .

To obtain a sufficient condition for the instability, one may use the condition for instability proposed by Ref. [33]

$$\int_{r_e(\alpha, P)}^{\infty} \left[\frac{V_e(r, \alpha, P, \lambda)}{g_e(r, \alpha, P)} \right] dr \equiv I(\alpha, P, \lambda) < 0. \quad (28)$$

This condition leads to

$$I(\alpha, P, \lambda) = \frac{2(11 \cdot 3^{3/4} \sqrt{\alpha P^2} + 26 \cdot 3^{1/3} \lambda)}{165(\alpha P^2)^{3/4}} < 0, \quad (29)$$

which is solved for $P > 0$ and $\lambda < 0$ as

$$0 < P \leq P_{\text{cqOSe}}(\lambda), \quad P_{\text{cqOSe}}(\lambda) = -\frac{26\lambda}{33\alpha}. \quad (30)$$

The sufficiently unstable region is depicted by the shaded region in Fig. 3(b). However, one could not obtain scalar cloud which is a seed to generate scalarized cqOSe-black holes. This is because its boundary potential [29]

$$V_{\text{eb}}(r, \alpha, P) = \frac{4}{\sqrt{3}r^6} \sqrt{\frac{-27(\alpha P^2)^2 + 30 \cdot 3^{1/4}(\alpha P^2)^{5/4}r^3 - 4\sqrt{3\alpha P^2}r^6}{g_e(r, \alpha, P)}}, \quad (31)$$

is not properly defined for outside the outer horizon [$r > 1.316 > r_+ (= 1.019)$] for $\lambda < 0$. This requires our investigation to confine to the near-extremal limit or the near-horizon approximation.

3.2 GB^{BR} scalarization to find scalar clouds

In the previous section, we did not obtain a numerical scalar cloud which might be a scalar seed for scalarized cqOSe-black hole in the single branch. Here, we wish to find analytic scalar clouds. For the cqOSe-black hole, one always finds its near-horizon geometry of the BR background ($\text{AdS}_2 \times S^2$) as [34]

$$ds_{\text{BR}}^2 = \frac{2}{g_e''(r_e)} \left(-\rho^2 d\tau^2 + \frac{d\rho^2}{\rho^2} \right) + r_e^2(d\theta^2 + \sin^2 \theta d\varphi^2), \quad (32)$$

where

$$\frac{2}{g_e''(r_e)} = \frac{(3\alpha P^2)^{1/4}}{2}, \quad r_e^2 = (3\alpha P^2)^{1/4}. \quad (33)$$

Here, two coordinates (τ, ρ) are dimensionless and the extremal horizon is located at $\rho = 0$.

Using Eq.(32), we compute the GB term to define its mass term (μ^2) as

$$-\lambda \mathcal{R}_{\text{GB}}^2 = \frac{16\lambda}{3\alpha P^2} \rightarrow \mu^2 \quad (34)$$

Then, s -mode linearized equation for $\delta\phi(\tau, \rho)$ is given by

$$-\frac{1}{\rho^2} \partial_\tau^2 \delta\phi + \partial_\rho(\rho^2 \partial_\rho \delta\phi) - \mu^2 \delta\phi = 0. \quad (35)$$

Introducing a tortoise coordinate $\rho_* = 1/\rho$, the s -mode scalar equation leads to [24]

$$-\frac{\partial^2 \delta\phi(\tau, \rho_*)}{\partial \tau^2} + \frac{\partial^2 \delta\phi(\tau, \rho_*)}{\partial \rho_*^2} = V_{\text{GB}}(\rho_*, \lambda) \delta\phi(\tau, \rho_*), \quad (36)$$

where the GB potential is given by

$$V_{\text{GB}}(\rho_*, \lambda) = \frac{\mu^2}{\rho_*^2} \rightarrow V_{\text{GB}}(\rho, \lambda) = \mu^2 \rho^2. \quad (37)$$

Now, we would like to mention the Breitenlohner-Freedman (BF) bound for a massive scalar propagating around AdS_2 spacetime [35, 36]

$$\mu^2 \geq \mu_{\text{BF}}^2 = -\frac{1}{4}. \quad (38)$$

For $\mu^2 < \mu_{\text{BF}}^2$ case, it corresponds to tachyon propagating around AdS_2 spacetime and this spacetime becomes unstable.

To obtain scalar clouds, it is important to solve the static scalar equation with $\omega = 0$

$$\frac{\partial^2 \delta\phi(\rho_*)}{\partial \rho_*^2} - V_{\text{GB}}(\rho_*, \lambda) \delta\phi(\rho_*) = 0. \quad (39)$$

One finds a scalar cloud

$$\delta\phi(\rho_*, \lambda) = c_1(\rho_*)^{\frac{1}{2}+\nu} + c_2(\rho_*)^{\frac{1}{2}-\nu} \rightarrow \delta\phi(\rho, \lambda) = c_1(\rho)^{-\nu-\frac{1}{2}} + c_2(\rho)^{\nu-\frac{1}{2}} \quad (40)$$

with

$$\nu = \frac{\sqrt{4\mu^2 + 1}}{2}. \quad (41)$$

Choosing $\mu^2 = -8$ ($\lambda = -3\alpha P^2/2 = -1.01$) and $c_1 = c_2 = 1/2$, the tachyonic seed and its potential are given by

$$\delta\phi(\rho, \mu^2 = -8) = \frac{1}{\sqrt{\rho}} \cos \left[\frac{\sqrt{31} \ln(\rho)}{2} \right], \quad V_{\text{GB}}(\rho, \mu^2 = -8) = -8\rho^2, \quad (42)$$

which has many nodes as is shown Fig. 4(a), but it takes a large value of 100 at $\rho = 10^{-4}$. This tachyonic cloud represents one (negative) branch for scalarization of cqOSe-black holes. To compare it with the conventional scalar clouds, one introduce regular (finite at the horizon) scalar clouds labelled by number of nodes ($n = 0, 1, 2, \dots$) for GB^+ scalarization of Schwarzschild black holes [see Fig. 4(b)]. These were obtained by solving static linearized equation numerically [37]: $\delta\phi_0(r, M = 1)$ has zero node (zero crossing at r -axis) with $n = 0$ branch point $\lambda_0 = 0.73$, $\delta\phi_1(r, M = 1)$ has one node with $n = 1$ branch point $\lambda_1 = 4.87$, and $\delta\phi_2(r, M = 1)$ has two nodes with $\lambda_2 = 12.8$.

Selecting $\mu^2 = 8$ ($\lambda = 3\alpha P^2/2 = 1.01$) with $c_1 = 1$ and $c_2 = 0$, one finds from Eq.(40) as

$$\delta\phi(\rho, \mu^2 = 8) = \rho^{-\frac{1}{2}(\sqrt{33}+1)}, \quad (43)$$

which shows that $\delta\phi(\rho, \mu^2 = 8)$ approaches infinity as $\rho \rightarrow 0$, but it is zero at $\rho = \infty$ without node (see Fig. 4(c)) and thus, it is called the blow-up scalar cloud at the horizon

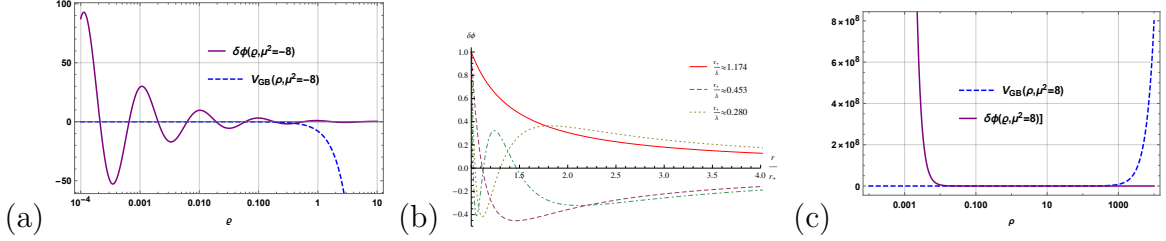


Figure 4: Three different scalar clouds. (a) Tachyonic scalar cloud of $\delta\phi(\rho, \mu^2 = -8)$ and its negative potential $V_{\text{GB}} = -8\rho^2$ with negative λ for GB^{BR} scalarization. This has many nodes but it has a large value as 100 at $\rho = 10^{-4}$. (b) Regular scalar clouds $\delta\phi_n(r, r_+ = 2)$ with $n = 0, 1, 2, 3$ for GB⁺ scalarization [37]. Here, n represents number of nodes (number of zero-crossings at r -axis). (c) Scalar cloud of $\delta\phi(\rho, \mu^2 = 8)$ which blows up as $\rho \rightarrow 0$ and its positive potential $V_{\text{GB}} = 8\rho^2$ with positive λ .

even though it is similar to the $n = 0$ branch in Fig. 4(b). This can represent the other (positive) branch. In addition, we note that the other form of $\rho^{\frac{1}{2}(\sqrt{33}-1)}$ approaches zero as $\rho \rightarrow 0$ while it takes the infinity as $\rho \rightarrow \infty$, corresponding to a non-normalizable solution.

Consequently, we find two scalar clouds for two branches of negative and positive λ , showing a feature of GB^{BR} scalarization for cqOSe-black holes. We notify that the positive branch arose from the BR ($\text{AdS}_2 \times S^2$) geometry.

4 Entropy function approach

Now, we perform entropy function approach [30] because the entropy is only the physical quantity to describe scalarized cqOSe black holes [38, 39]. The entropy function for the magnetically charged case is defined as [40]

$$\mathcal{E} = -2\pi \int_{S^2} d\theta d\varphi \left\{ \sqrt{-g} \mathcal{L}_{\text{EGBS-N}} \right\}, \quad (44)$$

where its metric and horizon quantities are given by

$$ds_{\text{br}}^2 = g_{\mu\nu} dx^\mu dx^\nu = v_1 \left(-\rho^2 d\tau^2 + \frac{d\rho^2}{\rho^2} \right) + v_2 (d\theta^2 + \sin^2 \theta d\varphi^2), \quad \phi = u, \quad F_{\theta\varphi} = p \sin \theta. \quad (45)$$

Here, v_1 and v_2 are two parameters to be determined. In this case, the entropy function leads to

$$\mathcal{E} = \pi \left[v_2 - v_1 + \frac{3v_1 \alpha p^2}{v_2^2} + 8 \left(\lambda u^2 - \zeta u^4 \right) \right]. \quad (46)$$

By extremizing this entropy function with respect to v_1 and v_2 , we find two relations

$$v_2 = \sqrt{3\alpha}p = r_e^2, \quad v_1 = \frac{\sqrt{3\alpha}p}{2} = \frac{v_2}{2}. \quad (47)$$

After eliminating v_1 from the entropy function in Eq.(46), one has the reduced form

$$\mathcal{E}_r = \pi \left[v_2 + 8 \left(\lambda u^2 - \zeta u^4 \right) \right], \quad (48)$$

which is the same form as that derived by the Wald entropy for $\phi = u$

$$S_{\text{Wald}} = -2\pi \oint \frac{\partial \mathcal{L}_{\text{EGBS-N}}}{\partial R_{\mu\nu\rho\sigma}} \epsilon_{\mu\nu} \epsilon_{\rho\sigma} r^2 d\Omega_2^2 |_{r=r_e}. \quad (49)$$

Extremizing \mathcal{E}_r with respect to scalar field u leads to

$$u = \sqrt{\frac{\lambda}{2\zeta}}, \quad (50)$$

which implies that $\phi = u$ is a secondary hair because it is determined by known coupling constants λ and ζ but not a new scalar charge q_s . Also, to get a real u , one requires the same sign for λ and ζ . Plugging Eq.(50) into Eq.(48), we find the final entropy function

$$\mathcal{E}_f(\alpha, p, \lambda, \zeta) = \pi \left(v_2 + \frac{2\lambda^2}{\zeta} \right) \rightarrow \pi \left(\sqrt{3\alpha}p + \frac{2\lambda^2}{\zeta} \right). \quad (51)$$

As is shown in Fig. 5, we have a sequence of entropy: $\mathcal{E}_f(\alpha = 1, p, \zeta = 2, \lambda = 1.01) > \mathcal{E}_f(1, p, 2, 0) > \mathcal{E}_f(1, p, -2, -1.01)$. This implies that a phase transition from cqOSe to scalarized cqOSe with $\lambda = 1.01$ may occur. For $p = 0.82$, one has $\mathcal{E}_f = 7.658(\lambda = 1.01)$, 4.462 for $\lambda = 0$, and $\mathcal{E}_f(1, 0.82, -2, -1.01) = 1.266$. where the first/last correspond to the entropy for two scalar clouds (two branches) of $\mu^2 = \pm 8$ in Fig. 4(a, c). For $\lambda = -1.01$, one finds that the positive entropy of $\mathcal{E}_f(1, p, -2, -1.01) > 0$ is obtained for $p > 0.5873$.

5 Discussions

We have investigated GB[−] scalarization of cqOSe-black hole in the EGBS theory with the NED term \mathcal{L}_{NED} . This extremal black hole is described by quantum α and magnetic charge P . Importantly, this is equivalent to the qOS-extremal black hole whose action (\mathcal{L}_{qOS}) is still unknown when imposing the relation between charge and mass $[(3\alpha P^2)^{1/4} \rightarrow 3M/2]$.

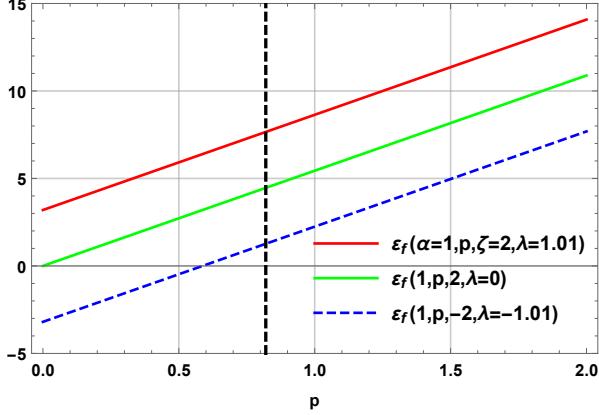


Figure 5: Entropy function $\mathcal{E}_f(\alpha = 1, p, \zeta = \pm 2, \lambda)$ with $\lambda = 1.01, 0, -1.01$ as a function of magnetic charge p for scqOSe- and cqOSe-black holes. The dashed line is located at $p = 0.82$. For $p = 0.82$, one has $\mathcal{E}_f(1, 0.82, 2, 1.01) = 7.658$, 4.462 for $\lambda = 0$, and $\mathcal{E}_f(1, 0.82, -2, -1.01) = 1.266$.

Studying on the onset of GB^- scalarization based on the linearized theory with coupling parameter λ , we expected to find the single branch of scalarized cqOS extremal (scqOSe)-black holes. However, we could not find its scalar cloud which is a seed to generate the single branch. To obtain scalar clouds, we consider its near-horizon geometry of the BR spacetime $(AdS_2 \times S^2)$. Two scalar clouds were found to represent two branches: One branch with $\lambda = -1.01$ is represented the tachyonic cloud with many nodes (but it takes a large value of 100 at the horizon $\rho = 10^{-4}$). The other branch with $\lambda 1.01$ is represented by the regular cloud without node (but it blows up at the horizon). The latter arose from the BR $(AdS_2 \times S^2)$ geometry.

We have applied Sen's entropy function approach to this theory with quartic coupling function $f(\phi) = 2(\lambda\phi^2 - \zeta\phi^4)$. If $\zeta = 0$, one cannot obtain scalar hair $u \neq 0$. We obtained the entropy function which shows the only physical quantity to describe the scqOSe-black holes. The $\lambda = \pm 1.01$ branches induce different entropy, leading to that $\lambda = 1.01$ branch is preferred than $\lambda = -1.01$ branch. Furthermore, we found that $\mathcal{E}_f(\alpha = 1, p, \zeta = 2, \lambda = 1.01)$ is greater than $\mathcal{E}_f(1, p, 2, \lambda = 0)$. This implies that a phase transition from cqOSe to scalarized cqOSe may occur.

6 Acknowledgments

The author is supported by the National Research Foundation of Korea (NRF) grant funded by the Korea government (MSIT) (RS-2022-NR069013).

References

- [1] J. Lewandowski, Y. Ma, J. Yang and C. Zhang, Phys. Rev. Lett. **130** (2023) no.10, 101501 doi:10.1103/PhysRevLett.130.101501 [arXiv:2210.02253 [gr-qc]].
- [2] A. Ashtekar, T. Pawłowski and P. Singh, Phys. Rev. Lett. **96** (2006), 141301 doi:10.1103/PhysRevLett.96.141301 [arXiv:gr-qc/0602086 [gr-qc]].
- [3] S. H. Mazharimousavi, Eur. Phys. J. C **85** (2025) no.6, 667 doi:10.1140/epjc/s10052-025-14410-8 [arXiv:2502.10457 [gr-qc]].
- [4] M. Skvortsova, Eur. Phys. J. C **85** (2025) no.8, 854 doi:10.1140/epjc/s10052-025-14589-w [arXiv:2411.06007 [gr-qc]].
- [5] S. H. Dong, F. Hosseini Far, F. Studnička and H. Hassanabadi, Phys. Lett. B **860** (2025), 139182 doi:10.1016/j.physletb.2024.139182
- [6] G. Panotopoulos and F. Tello-Ortiz, Phys. Lett. B **868** (2025), 139769 doi:10.1016/j.physletb.2025.139769 [arXiv:2507.22945 [gr-qc]].
- [7] J. Yang, C. Zhang and Y. Ma, Eur. Phys. J. C **83** (2023) no.7, 619 doi:10.1140/epjc/s10052-023-11800-8 [arXiv:2211.04263 [gr-qc]].
- [8] J. P. Ye, Z. Q. He, A. X. Zhou, Z. Y. Huang and J. H. Huang, Phys. Lett. B **851** (2024), 138566 doi:10.1016/j.physletb.2024.138566 [arXiv:2312.17724 [gr-qc]].
- [9] L. Chen and S. Jiang, Phys. Lett. B **866** (2025), 139522 doi:10.1016/j.physletb.2025.139522
- [10] Y. S. Myung, Eur. Phys. J. C **85** (2025) no.7, 745 doi:10.1140/epjc/s10052-025-14472-8 [arXiv:2505.19450 [gr-qc]].
- [11] C. Charmousis, B. Gouteraux, B. S. Kim, E. Kiritsis and R. Meyer, JHEP **11** (2010), 151 doi:10.1007/JHEP11(2010)151 [arXiv:1005.4690 [hep-th]].
- [12] M. Angheben, M. Nadalini, L. Vanzo and S. Zerbini, JHEP **05** (2005), 014 doi:10.1088/1126-6708/2005/05/014 [arXiv:hep-th/0503081 [hep-th]].

- [13] M. Volonteri, P. Madau, E. Quataert and M. J. Rees, *Astrophys. J.* **620** (2005), 69-77 doi:10.1086/426858 [arXiv:astro-ph/0410342 [astro-ph]].
- [14] L. Gou, J. E. McClintock, R. A. Remillard, J. F. Steiner, M. J. Reid, J. A. Orosz, R. Narayan, M. Hanke and J. García, *Astrophys. J.* **790** (2014) no.1, 29 doi:10.1088/0004-637X/790/1/29 [arXiv:1308.4760 [astro-ph.HE]].
- [15] B. Carter, *Phys. Rev. Lett.* **26** (1971), 331-333 doi:10.1103/PhysRevLett.26.331
- [16] R. Ruffini and J. A. Wheeler, *Phys. Today* **24** (1971) no.1, 30 doi:10.1063/1.3022513
- [17] C. A. R. Herdeiro and E. Radu, *Int. J. Mod. Phys. D* **24** (2015) no.09, 1542014 doi:10.1142/S0218271815420146 [arXiv:1504.08209 [gr-qc]].
- [18] D. D. Doneva and S. S. Yazadjiev, *Phys. Rev. Lett.* **120** (2018) no.13, 131103 doi:10.1103/PhysRevLett.120.131103 [arXiv:1711.01187 [gr-qc]].
- [19] H. O. Silva, J. Sakstein, L. Gualtieri, T. P. Sotiriou and E. Berti, *Phys. Rev. Lett.* **120** (2018) no.13, 131104 doi:10.1103/PhysRevLett.120.131104 [arXiv:1711.02080 [gr-qc]].
- [20] G. Antoniou, A. Bakopoulos and P. Kanti, *Phys. Rev. Lett.* **120** (2018) no.13, 131102 doi:10.1103/PhysRevLett.120.131102 [arXiv:1711.03390 [hep-th]].
- [21] C. A. R. Herdeiro, E. Radu, N. Sanchis-Gual and J. A. Font, *Phys. Rev. Lett.* **121** (2018) no.10, 101102 doi:10.1103/PhysRevLett.121.101102 [arXiv:1806.05190 [gr-qc]].
- [22] Y. S. Myung and D. C. Zou, *Eur. Phys. J. C* **79** (2019) no.3, 273 doi:10.1140/epjc/s10052-019-6792-6 [arXiv:1808.02609 [gr-qc]].
- [23] D. D. Doneva, F. M. Ramazanoğlu, H. O. Silva, T. P. Sotiriou and S. S. Yazadjiev, *Rev. Mod. Phys.* **96** (2024) no.1, 015004 doi:10.1103/RevModPhys.96.015004 [arXiv:2211.01766 [gr-qc]].
- [24] Y. Brihaye and B. Hartmann, *Phys. Lett. B* **792** (2019), 244-250 doi:10.1016/j.physletb.2019.03.043 [arXiv:1902.05760 [gr-qc]].
- [25] C. A. R. Herdeiro, A. M. Pombo and E. Radu, *Universe* **7** (2021) no.12, 483 doi:10.3390/universe7120483 [arXiv:2111.06442 [gr-qc]].

[26] Y. S. Myung, Eur. Phys. J. C **85** (2025) no.11, 1327 doi:10.1140/epjc/s10052-025-15063-3 [arXiv:2509.24113 [gr-qc]].

[27] M. Richartz, Phys. Rev. D **93** (2016) no.6, 064062 doi:10.1103/PhysRevD.93.064062 [arXiv:1509.04260 [gr-qc]].

[28] D. Senjaya, Eur. Phys. J. C **85** (2025) no.9, 1012 doi:10.1140/epjc/s10052-025-14711-y

[29] S. Hod, Eur. Phys. J. C **77** (2017) no.5, 351 doi:10.1140/epjc/s10052-017-4920-8 [arXiv:1705.04726 [hep-th]].

[30] A. Sen, JHEP **09** (2005), 038 doi:10.1088/1126-6708/2005/09/038 [arXiv:hep-th/0506177 [hep-th]].

[31] K. A. Meissner, Class. Quant. Grav. **21** (2004), 5245-5252 doi:10.1088/0264-9381/21/22/015 [arXiv:gr-qc/0407052 [gr-qc]].

[32] M. Domagala and J. Lewandowski, Class. Quant. Grav. **21** (2004), 5233-5244 doi:10.1088/0264-9381/21/22/014 [arXiv:gr-qc/0407051 [gr-qc]].

[33] G. Dotti and R. J. Gleiser, Class. Quant. Grav. **22** (2005), L1 doi:10.1088/0264-9381/22/1/L01 [arXiv:gr-qc/0409005 [gr-qc]].

[34] M. de Cesare, R. Oliveri and A. P. Porfyriadis, Phys. Rev. D **111** (2025) no.4, 044028 doi:10.1103/PhysRevD.111.044028 [arXiv:2410.23446 [gr-qc]].

[35] P. Breitenlohner and D. Z. Freedman, Annals Phys. **144** (1982), 249 doi:10.1016/0003-4916(82)90116-6

[36] P. Breitenlohner and D. Z. Freedman, Phys. Lett. B **115** (1982), 197-201 doi:10.1016/0370-2693(82)90643-8

[37] Y. S. Myung and D. C. Zou, Phys. Rev. D **98** (2018) no.2, 024030 doi:10.1103/PhysRevD.98.024030 [arXiv:1805.05023 [gr-qc]].

[38] A. Marrani, O. Miskovic and P. Quezada Leon, JHEP **02** (2018), 080 doi:10.1007/JHEP02(2018)080 [arXiv:1712.01425 [hep-th]].

- [39] A. Marrani, O. Miskovic and P. Q. Leon, JHEP **07** (2022), 100
doi:10.1007/JHEP07(2022)100 [arXiv:2203.14388 [hep-th]].
- [40] Y. S. Myung, Y. W. Kim and Y. J. Park, Phys. Rev. D **76** (2007), 104045
doi:10.1103/PhysRevD.76.104045 [arXiv:0707.1933 [hep-th]].